

# Surface modification of corona treated poly(ethylene terephthalate) film: adsorption and wettability studies

B. Leclercq and M. Sotton

*Institut Textile de France, 35 rue des Abondances, 92100 Boulogne, France*

and A. Baszkin and L. Ter-Minassian-Saraga

*Laboratoire de Physico-Chimie des Surfaces, UER Biomédicale 81, Université René Descartes,*

*45, rue des Saints-Pères, 75006 Paris, France*

*(Received 10 January 1977; revised 15 February 1977)*

Corona discharge treatment of poly(ethylene terephthalate) (PET) films produces chemical and physical modification of the surface leading to the formation of cavities and bumps. The roughness of the surface increases with the time of treatment and may be detected by scanning electron microscopy for the samples treated above 10 cycles, which corresponds to the duration of the exposure of the film under the electrodes. The degree of chemical modification, producing OH groups, is observed by adsorption of radioactive calcium ions and contact angle measurements. The results of these measurements are discussed and evidence presented shows that increase of the surface density of functional groups up to the value of  $0.2 \times 10^{14}$  sites/cm<sup>2</sup> leads to a rapid increase in wettability of PET films.

## INTRODUCTION

It is known that electrical discharge modifies the physical and chemical nature of polymer surfaces and in general enhances their wettability towards liquids and their adhesion to other materials. This effect may also be obtained by chemical treatment. In polyethylene films treated by a mixture of sulphuric acid and potassium chlorate, carbonyl groups are produced at the surface of the polymer and these may be determined quantitatively by adsorption of radioactive calcium ions. The degree of oxidation thus obtained may be related to the increase of solid-liquid free energy of adhesion<sup>1</sup>.

The corona discharge treatment does not modify the mechanical properties of wood fibres, but increases the resilience of yarns as compared to those of the same twist made out of the untreated fibres. The result of this is a higher dimensional stability of the cloth and an increase of the fibre-resin adhesivity coefficient<sup>2-6</sup>. It was also found that corona-treated wool contains oxidation products, mainly in the cuticle layer, resulting from transformation of the amino-acid cystin into cysteic acid by cleavage of disulphur bonds<sup>5</sup>. The tenacity of cotton yarns is increased by a similar treatment<sup>7</sup>. Cellulose, polyethylene and polyester films exhibit strong self-adhesion after corona treatment and when joined together under conditions of heat and pressure<sup>8-12</sup>.

The new properties of the surface induced by the treatment may be explained either by the change of surface topography or by the formation of additional functional sites. These effects may be complementary to each other.

The purpose of this work was to study the adsorption and wetting behaviour of poly(ethylene terephthalate) (PET) films in order to distinguish the above two effects. The PET films were preferred rather than fibres so as to make the experiments easier.

## EXPERIMENTAL

### Materials

Poly(ethylene terephthalate) PET film, known under the commercial name Terphane and produced by Cellophane, was used for this work. It has a thickness of 35  $\mu$ m and, before the corona treatment, was extracted with ethanol. Dried circular samples of the film, 30 mm in diameter, were used for the adsorption and contact angle measurements. Water was tri-distilled from a permanganate solution using Pyrex apparatus. Its surface tension was 72.75 dyne/cm. <sup>45</sup>Ca calcium chloride was obtained from the Commissariat à l'Energie Nucléaire, France. Solutions of different concentrations of CaCl<sub>2</sub> with the specific activity 440 mCi/g were prepared using 10<sup>-3</sup> M NaOH to keep the ionic strength constant.

### Methods

**Electrical discharge.** The corona discharge cell with two electrodes is shown in Figure 1. One of these electrodes (A) with an inverted T shape, made of aluminium and with dimensions  $a = 25$  mm,  $b = 250$  mm, is supplied by an alternating high voltage. The second electrode, in the form of a roller (B), 200 mm in diameter and overlapped with dielectric, is earth connected. The gap between the electrodes is

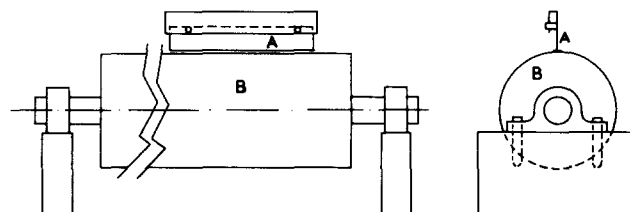


Figure 1 Electrical corona discharge cell

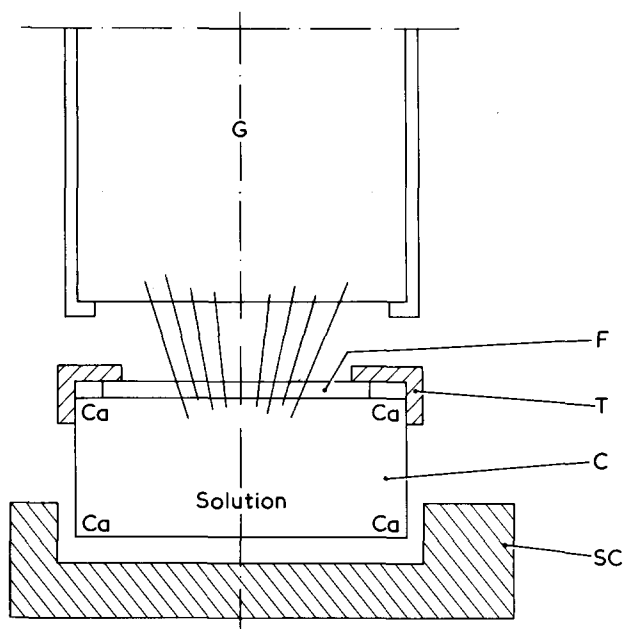


Figure 2 Adsorption measuring apparatus. G, Geiger-Müller tube; F, PET film; T, Teflon window; C, crystallizing dish; SC support

adjusted to 0.8 mm. PET film is stuck to the roller by means of adhesive tape. The rotary motion of the roller assures the change of sample surface submitted to the corona treatment and the time during which the sample of PET film is under the electrical discharge.

During all the experiments reported here, the frequency of the current was 20 kHz and the tension applied to the electrodes was 16 kV. The rotation speed of the roller was 24 cycles/min. The time of the corona discharge corresponded to the number of cycles performed by the roller, which varied from 1 to 1000.

**Sand abrasion.** PET films were sand abraded under two different pressures, 1.5 bar and 2.5 bar (1 bar =  $10^5$  N/m<sup>2</sup>). Samples of these films were prepared for electron microscopy examination and contact angle measurements.

**Adsorption measurements.** To determine the surface density of the polar sites created during the corona treatment of PET films, a radio tracer method was used<sup>13</sup>. The apparatus is shown in Figure 2. A circular sample of PET film is carefully placed at the surface of calcium chloride solution which fills up a dish (C). The dish, fixed in the support (SC), is covered with a Teflon window (T) and placed under the Geiger-Müller counting device (G). The whole apparatus is put into a chamber at a constant temperature of 23°C under saturated vapour pressure. To measure the radioactivity, the counter window is brought into contact with the Teflon window (T) in such a way that a perfect superposition can be obtained. The geometry of the system and the reproductibility of the measurements may thus be assured. A graphical recorder connected with the counting device enables one to follow the kinetics of adsorption and the time necessary to reach equilibrium. The amount of Ca<sup>2+</sup> ion adsorbed at a given PET/solution interface is deduced from the radioactivity *A*, measured above the PET film. The value of *A* includes the radioactivity *A<sub>F</sub>* originating from the adsorbed Ca<sup>2+</sup> ions, and *A<sub>0</sub>* from those of the superficial layer of the aqueous solution:  $A = A_F + A_0$ . For each calcium chloride concentration the *A<sub>0</sub>* radioactivity is measured with the untreated PET film

which does not exhibit any adsorption. The values of *A* for the treated PET films are obtained under the same geometrical conditions of the counting device. The radioactivity *A* (counts/min) has now to be converted to the amount of adsorption (ions Ca<sup>2+</sup>/cm<sup>2</sup>), i.e. the surface density of the created polar sites.

To obtain the corresponding conversion factor *f*, a solution containing a known amount of radioactive ions was deposited on a plane glass surface and evaporated. When dried (solid source) was covered with a PET film and its radioactivity determined under the same geometrical conditions as that of the adsorption measurements. If *n* is the quantity of deposited molecules of CaCl<sub>2</sub>, and *S* is the glass surface facing the counter, one may define the surface density as  $\delta = n/S$ . In order to improve the accuracy of the conversion factor *f*, one has to establish the counting curve between  $\delta = n/S$  and *A<sub>S</sub>*, where *A<sub>S</sub>* (in counts/min) is the radioactivity of the solid source. The slope of this curve, passing through the origin, gives *f*. Such a curve is represented in Figure 3.

#### Contact angle measurements

The apparatus for contact angle measurements used in this study consists of the following parts.

(a) The dark room chamber, double enclosed, thermostatted by means of an external liquid circuit. The chamber has two opposite windows and is installed on a plate allowing its displacement in two perpendicular horizontal directions. The sample holder inside the chamber is fixed above the small dish filled with water. This allows saturation of the air phase with the vapour and avoids evaporation of the liquid drop during the measurement.

(b) An exterior screw allowing rotation of the sample holder and measurement of contact angles on various sites of the sample surface.

(c) A microsyringe fixed at the top of the chamber by means of which a liquid drop of a known volume may be placed on the polymer surface. The microsyringe may be displaced in two opposite directions, thus ensuring deposition of the drop along the surface of the sample.

(d) A cathetometer with  $\times 15$  magnification, equipped with a goniometer allowing reading of contact angle.

The values of contact angle reported in this paper are an average of at least ten readings.

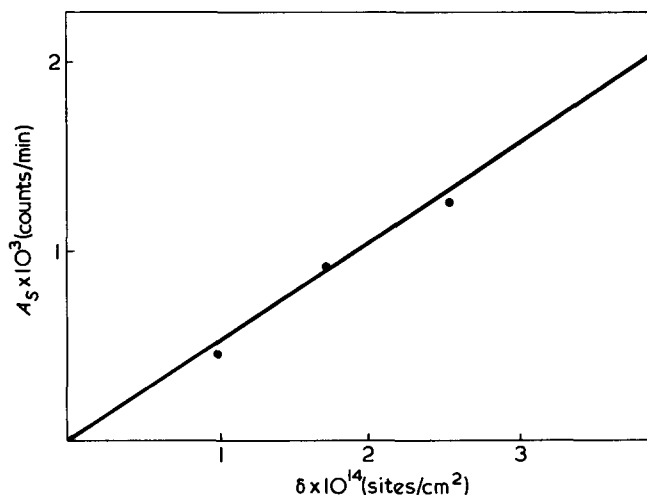


Figure 3 Radioactivity/surface density conversion curve

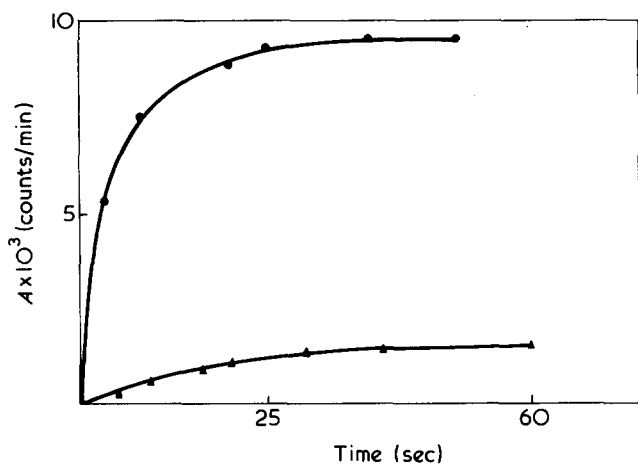


Figure 4 Kinetics of calcium ion adsorption on corona-treated PET films. Treatment time corresponding to 1000 cycles.  $\text{CaCl}_2$  concentration:  $\blacktriangle$ ,  $10^{-6}$  M;  $\bullet$ ,  $2 \times 10^{-5}$  M

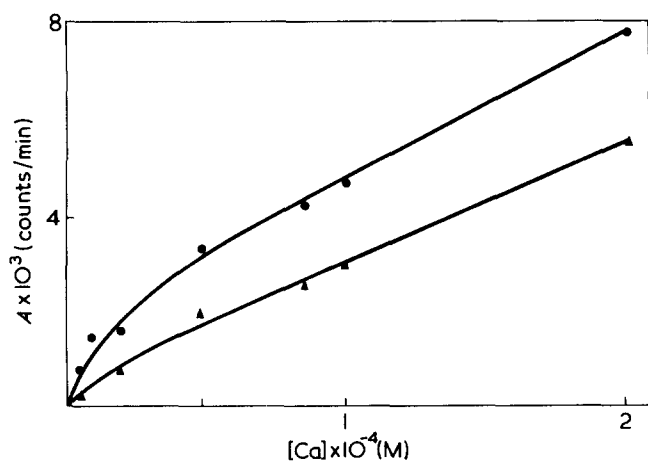


Figure 5  $\text{Ca}^{2+}$  adsorption at ( $\blacktriangle$ ) untreated PET film and at ( $\bullet$ ) PET corona-treated film (1000 cycles)

#### Scanning electron microscopy

The electron micrographs of the corona-treated and sand abraded PET films were obtained using a Cambridge Stereoscan microscope.

## RESULTS

### Adsorption of calcium ions on corona-treated PET films

Figure 4 shows the kinetics of adsorption of  $\text{Ca}^{2+}$  ions on corona-treated PET films for two different concentrations of calcium chloride in solution:  $10^{-6}$  M and  $2 \times 10^{-5}$  M. The time of treatment is 1000 cycles. It may be noticed that adsorption increases with the increase of  $\text{CaCl}_2$  concentration and that equilibrium is attained after 45 mins. For the same time of treatment (1000 cycles) the measured radioactivity is plotted against  $\text{CaCl}_2$  concentration in solution and compared to that of the untreated film (Figure 5). The difference in radioactivity is due to the interfacial adsorption. Figure 6 represents the isotherm of adsorption derived from the two curves of Figure 5 converted to the surface density  $\delta$ . It can be seen that the plateau value corresponding to the saturation of adsorption is obtained when the calcium concentration in solution is equal to  $10^{-4}$  M.

An experimental variation of the surface density of polar sites with the time of corona treatment is given in Figure 7.

The most remarkable feature of this Figure is that the polar sites are created after a very short exposure to the electrical discharge, below 10 cycles. It also indicates that the  $\delta$  value does not change significantly between 10 and 500 cycles and only increases for times of treatment greater to 500.

#### Contact angles

Figure 8 represents the variation of contact angle with

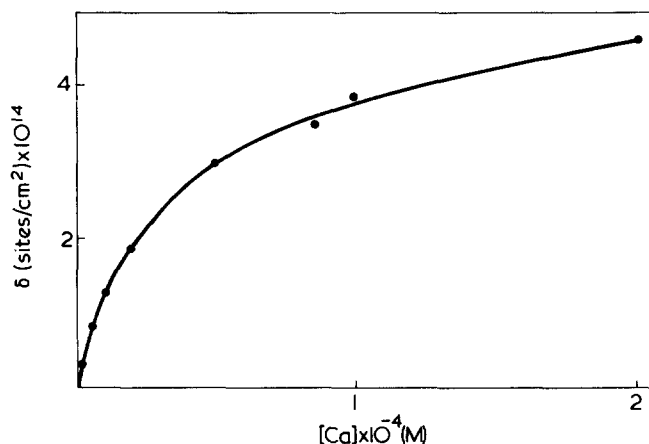


Figure 6 Isotherm of  $\text{Ca}^{2+}$  adsorption at PET corona-treated film (1000 cycles)

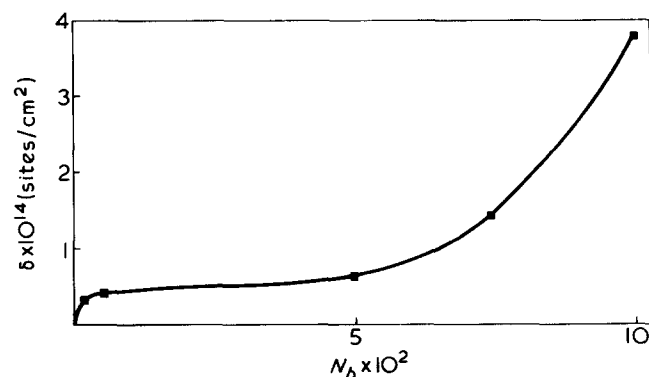


Figure 7 Surface density of polar groups versus treatment time ( $N_b$ ) = number of cycles). Conditions:  $[\text{Ca}] = 10^{-4}$  M,  $\text{pH} = 10$ ,  $[\text{Na}] = 10^{-3}$  M

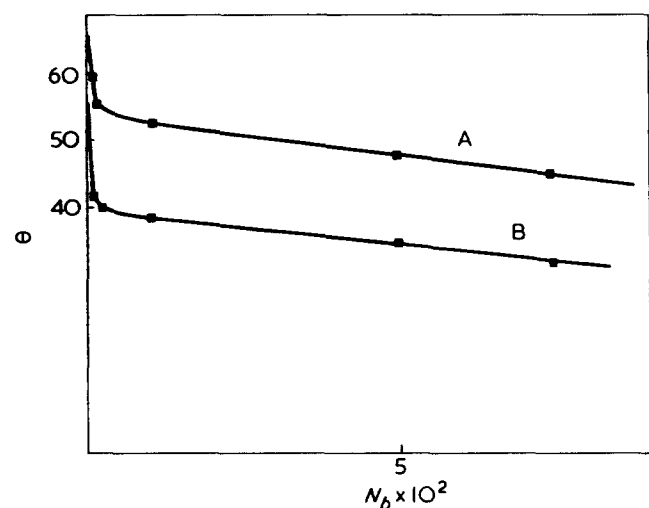


Figure 8 Contact angles (A,  $\theta_A$  advancing; B,  $\theta_r$  receding) versus treatment time

time of corona treatment. Two angles are recorded, advancing ( $\theta_A$ ) and receding ( $\theta_r$ ). Another representation of the wettability of corona-treated PET films is shown in Figure 9. Here the reversible work of adhesion of the liquid to the solid when coated with an adsorbed film of the saturated vapour is calculated by means of the Young–Dupré equation<sup>14</sup>.  $W_A = \gamma_{LV} (1 + \cos \theta)$ , and plotted versus the surface density of polar groups  $\delta$ . For calculation the surface tension of water,  $\gamma_{LV}$ , was taken<sup>15</sup> to be equal to 72.75 dyne/cm and  $\theta$  was the advancing contact angle. One can observe a pronounced fall of contact angle (Figure 8) e.g. the increase of solid–liquid work of adhesion (Figure 9) corres-

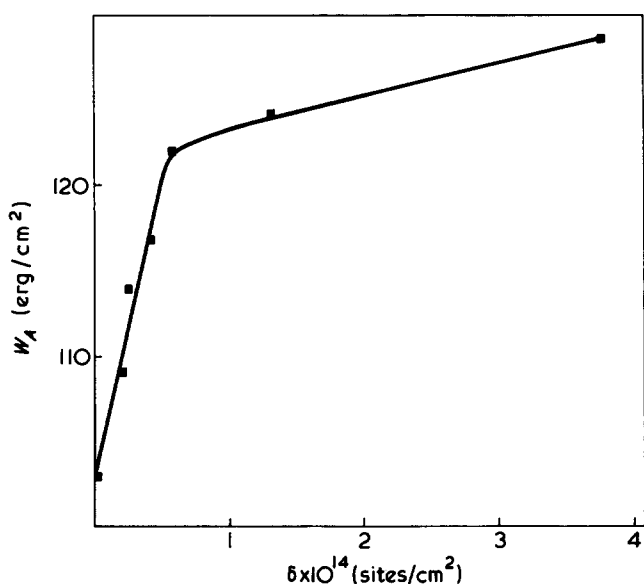


Figure 9 Work of adhesion versus density of polar groups (for  $\theta_A$ )

ponding to a short exposure time of PET films to corona discharge treatment.

Contact angles on sand abraded films are summarized in Table 1. The advancing contact angle on sand abraded PET films (pressure 2.5 bar) could not be obtained. This is due to the high degree of porosity of the surface, so that the capillarity effect may interfere.

#### Microscopic studies

Scanning electron micrographs of untreated and corona-treated films are given in Figure 10.

Examination of these micrographs reveals that the increase of the roughness for one cycle treated films, on a scale below the resolving power available, could not be distinguished. The Figures also show a gradual increase of roughness with time of discharge treatment, leading to the formation of cavities and hills.

The surface topography of sand abraded films is illustrated in Figure 11. It may also be noted that the more severe are the conditions of abrasion, the more pronounced is the surface roughness and the loss of polymer substance.

#### DISCUSSION

Several deductions can be drawn from the results obtained. The isotherm of calcium adsorption (Figure 6) is of the

Table 1 Contact angles:  $\theta_A$  (advancing),  $\theta_r$  (receding) of sand abraded PET films

	$\theta_A$	$\theta_r$
Untreated PET film	65.5	56.5
Sand abraded film (pressure 1.5 bar)	69	56
Sand abraded film (pressure 2.5 bar)		57

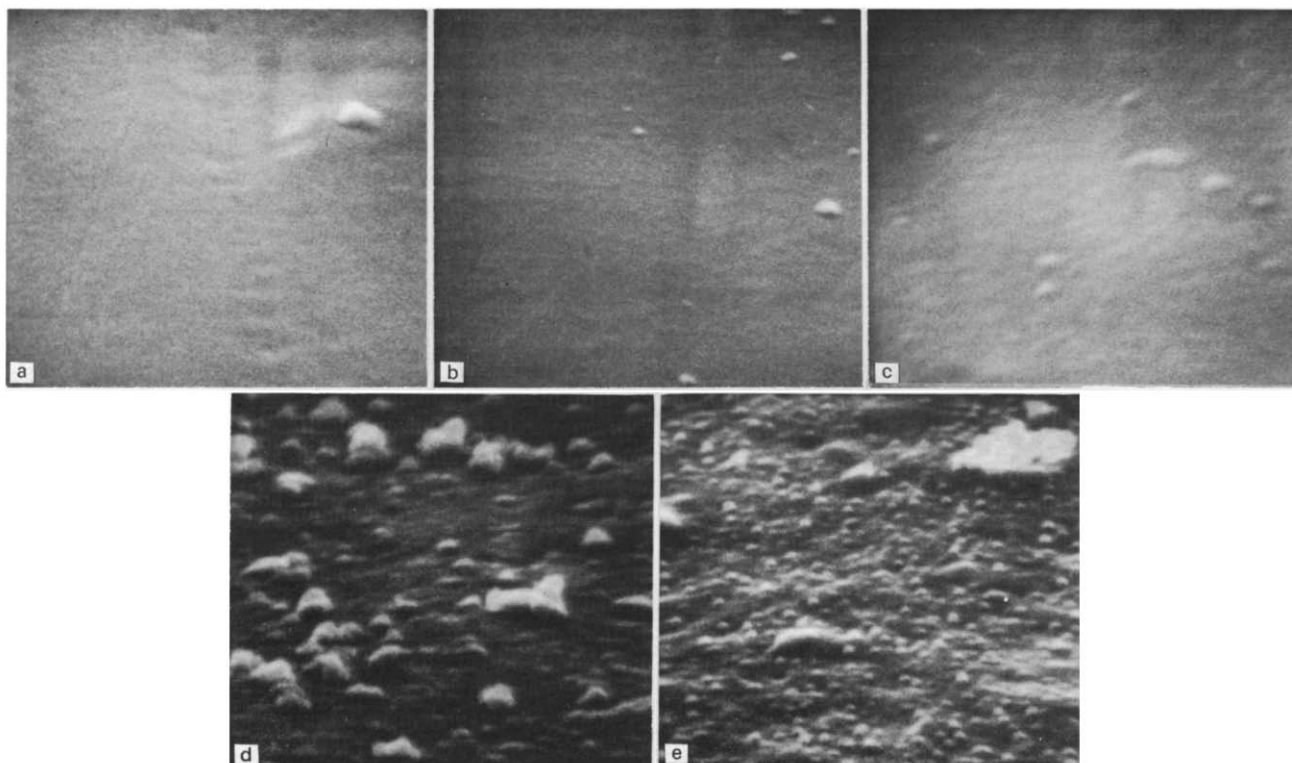


Figure 10 Photomicrographs of PET corona-treated film (a) Untreated film X 50 000; (b) 1 cycle X 50 000; (c) 10 cycles X 50 000, (d) 500 cycles X 50 000; (e) 1000 cycles X 50 000



This supposition seems to be justified, since the phenolic hydrogens which exhibit acidic behaviour may be easily substituted by an inorganic cation, especially at high pH.

In analysing the data of adsorption illustrated by Figure 7 we see that the flat part of the curve (10–500 cycles) corresponds to a  $\delta$  value equal to  $0.4 \times 10^{14}$  sites/cm<sup>2</sup>. This means that one adsorption site occupies an average area of 250 Å<sup>2</sup>. The unit cell of PET polymer has the dimensions<sup>18</sup>:  $a = 4.56$  Å,  $b = 5.94$  Å,  $c = 10.75$  Å and the area of the unit plane in its longitudinal direction is 64 Å<sup>2</sup>.

Taking into account the scission of the polymer chain during corona treatment leading to the creation of *para* and *meta* OH groups on the chain ends, 250 Å<sup>2</sup> for one site is a reasonable value. It also seems reasonable to think that the plateau value in Figure 7 (10–500 cycles) is due to saturation of the surface of treated PET film with OH groups. This is supported by the fact that the contact angle value practically does not change in this range of treatment time (Figure 8). Indeed, it is known from solid–solid<sup>11,12</sup> and liquid–solid<sup>15,19,20</sup> studies that the orientation of the functional groups contributing to adhesion is one of the most important factors. When the functional groups change their orientation from perpendicular to the surface towards the solid bulk or to their horizontal position, reduction in adhesion takes place immediately. If the surface is very porous and the functional groups in the cavities are not perpendicular to the liquid in contact, the same effect may be observed.

The shift of calcium adsorption (Figure 7) above 500 cycles needs further explanation. If the number of OH groups of the surface remained constant, what could then be the cause of the increase of calcium adsorption? The answer to this question may be found from careful examination of the photomicrographs. The surface roughness of corona-treated films becomes more and more pronounced and what we measure by calcium adsorption above 500 cycles is probably the contribution of OH groups both from the surface and in cavities. Contact angle measurements confirm this suggestion. Indeed, contact angle values do not change in the range 500–1000 cycles, indicating that the OH groups in contact with a liquid at the surface of polymer are at saturation.

The slope of Figure 9,  $\Delta W_A/\Delta\delta$  equal to  $35.6 \times 10^{-14}$  erg/site and corresponding to 5.14 kcal/mol, would represent the change of surface properties of PET films obtained during the treatment.

This value of the molar energy (5.14 kcal/mol) is in good agreement with that normally attributed<sup>21</sup> to hydrogen bond energy for numerous substances ( $\approx 5$  kcal/mol) and is superior to that found<sup>15</sup> with chemically oxidized polyethylene (2.52 kcal/mol). This result is not surprising, as the magnitude of the hydrogen bond molar energy with OH groups at the surface of PET films should be considerably higher than that of C = O groups of oxidized polyethylene.

Another important point requires discussion here. If we consider simultaneously the rapid creation of new functional groups for short corona-treatment times and a relatively small change of the surface porosity of these samples, the relationship between the increase of the wetting energy and surface density of functional groups can be established independently from the surface morphology. This would mean that the roughness effect does not influence the observed

increase of wettability. To prove such a statement, experiments have been made with the sand abraded films (Figure 11 and Table 1).

Our results, summarized in Table 1, show that the effect of the roughness on the wettability of sand abraded PET films is the same as that reported by Dettre and Johnson<sup>22</sup>. Following their findings the advancing contact angle increases to a certain limiting value with the increase of roughness, while the receding angle, passing initially through a minimum value, approaches a limit which is superior to the value found for a smooth surface.

These observations indicate that when only physical modifications of the polymer surface takes place the solid–liquid work of adhesion decreases. This is contrary to the phenomenon occurring during corona treatment of PET surfaces, where the solid–liquid work of adhesion increases. We may conclude, therefore, that the increase in the wetting energy enhanced by corona treatment is due only to the creation of superficial functional groups and not to the change of the surface morphology.

It follows that for films used in industry, when the times of treatment are less than one cycle (i.e.  $\delta < 0.2 \times 10^{14}$  sites/cm<sup>2</sup>) a further effort in the elaboration of measuring techniques should be made to control the number of functional groups.

## REFERENCES

- 1 Baszkin, A. and Ter-Minassian-Saraga, L. *J. Polym. Sci. (C)* 1971, **34**, 242
- 2 Kassenbeck, P. *Bull. Inst. Text. Fr.* 1974, **110**, 7
- 3 Thorsen, W. J. and Landwehr, R. C. *Text. Res. J.* 1971, **41**, 264
- 4 Thorsen, W. J. *J. Polym. Sci. Polym. Symp.* 1971, **18**, 1171
- 5 Guyennet, J. F., Jacquemart, J. and Leclercq, B. *Bull. Sci. Inst. Text. Fr.* 1974, **12**, 337
- 6 Jacquemart, J., Leclercq, B., Mazingue, G. and Ponchel, P. *Bull. Inst. Text. Fr.* 1975, **13**, 25
- 7 Belin, R. E. *J. Text. Inst.* 1976, **718**, 249
- 8 Goring, D. A. I. and Suranyi, G. *Pulp Pap. Can.* 1969, **20**, 390
- 9 Kim, C. Y. and Goring, D. A. I. *J. Appl. Polym. Sci.* 1971, **15**, 1357
- 10 Kim, C. Y., Evans, J. and Goring, D. A. I. *J. Appl. Polym. Sci.* 1971, **15**, 1365
- 11 Owens, D. K. *J. Appl. Polym. Sci.* 1975, **19**, 265
- 12 Owens, D. K. *J. Appl. Polym. Sci.* 1975, **19**, 3315
- 13 de Heaulme, M., Hendrikx, Y., Luzzati, A. and Ter-Minassian-Saraga, L. *J. Chim. Phys.* 1967, **64**, 1363
- 14 Zisman, W. A. *Adv. Chem. Ser.* 1964, **43**, 4
- 15 Baszkin, A., Nishino, M. and Ter-Minassian-Saraga, L. *J. Colloid Interface Sci.* 1976, **54**, 317
- 16 Valk, G., Kehren, M. L. and Daamen, I. *Angew. Makromol. Chem.* 1970, **13**, 97
- 17 Marcotte, F. B., Campbell, D., Cleaveland, J. A. and Turner, D. T. *J. Polym. Sci. (A-1)* 1967, **5**, 481
- 18 de Daubeny, R., Bunn, C. W. and Brown, C. J. *Proc. Roy. Soc. London (A)* 1954, **226**, 531
- 19 Baszkin, A. and Ter-Minassian-Saraga, L. *Polymer* 1974, **15**, 759
- 20 Baszkin, A., Deyme, M., Nishino, M. and Ter-Minassian-Saraga, L. *Prog. Colloid Polym. Sci.* 1976, **61**, 97
- 21 Ketelaar, J. A. in 'Liaisons et propriétés chimiques', Dunod, Paris, 1960, pp 348
- 22 Dettre, R. H. and Johnson, R. E. Jr. *Adv. Chem. Ser.* 43, American Chemical Society, Washington, D.C. 1964, 136